Journal of Hydrology: Regional Studies 53 (2024) 101769

Contents lists available at ScienceDirect

Journal of Hydrology: Regional Studies

journal homepage: www.elsevier.com/locate/ejrh

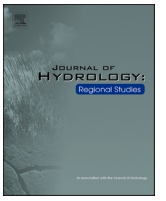

Delineating the predominant impact of rising temperature on the enhancement of severity in compound drought-hot events in China: An empirical Copula and path analysis-based approach

Xiaohua Xiang [a], Yongxuan Li [a], Xiaoling Wu [a,*], Hongwei Cao [b], Xian Lin [b]

[a] College of Hydrology and Water Resources, Hohai University, Nanjing, PR China
[b] China Yangtze Power Co. Ltd., Yichang, PR China

ARTICLE INFO

Keywords:
Compound drought-hot events
Copula
Path analysis
Climate change
Water deficit

ABSTRACT

Study region: China
Study focus: Compound drought-hot events (CDH) inflict serious socio-economic damages on our society and the natural environment. Given the inverse relationship between average summer temperature and precipitation, this investigation introduces an innovative empirical copula-based compound drought-hot index (CDHI). This index is crafted from the joint distribution of the standardized precipitation evapotranspiration index (SPEI) and standardized temperature index (STI). While previous research has documented a rising trend in these complex events on both regional and global stages, scrutiny into their escalating severity remains limited. To highlight the critical role of climbing temperatures in the increasing severity of CDH events within China, our research utilizes the CDHI in tandem with a path analysis to precisely assess severity shifts in CDH occurrences during the warm season from 1901 to 2022.
New hydrological insights for the region: This study used an empirical copula-based CDH index and implemented the path analysis to quantify the response of severity changes of compound drought-hot events to shifts of summer mean temperature and water deficit from the historical perspective. Our findings reveal a marked escalation in CDH severity across much of China. Path analysis divulges that the influence of rising summer temperatures on CDH severity has seen a significant uptick in the last 60 years (1962–2022), displaying a more considerable contribution rate than the earlier 60-year span (1901–1961). This points to the changing impact of temperature on CDH events over recent decades. During the initial interval (1901–1961), we saw a 0.7% and 1.7% per-decade increase in areas affected by severe and moderate CDH events, respectively. Contrastingly, the subsequent period (1962–2022) experienced a more significant rise, with the area affected by severe and moderate events expanding over twice as much. Totally speaking, this exploration enhances our comprehension of the intensification in CDH event severity and the role of climatic drivers. These insights can contribute to improved risk assessments and the development of tailored adaptation and mitigation strategies in the face of ongoing climate change.

* Corresponding author.
E-mail address: freebir7237@hhu.edu.cn (X. Wu).

https://doi.org/10.1016/j.ejrh.2024.101769
Received 4 January 2024; Received in revised form 21 February 2024; Accepted 29 March 2024
Available online 1 April 2024

1. Introduction

The scholarly community widely acknowledges a marked escalation in the probability of extreme weather and climate events at a worldwide or regional scale (Zscheischler et al., 2018; Alizadeh et al., 2020; AghaKouchak et al., 2021; Yuan et al., 2023; Xu et al., 2023a), events which yield substantive negative and unevenly distributed consequences for societies and ecosystems. In the context of an increasingly warm climate, the incidence of severe droughts and heat events has risen across the globe's land areas in recent decades (Kirono et al., 2017; Zhou and Liu, 2018; Xu et al., 2023b). Among these, numerous drought instances have been recorded occurring alongside hot events (Griffin and Anchukaitis, 2014; Sedlmeier et al., 2017; Feng et al., 2020; Zamora-Reyes et al., 2022), which are often defined as "compound drought-hot events (CDH)." Xu et al. (2023a) and (2023b) have verified the merits of copulas to measure the overall severity of compound droughts and hot extremes by taking into account the dependence structure of multiple contributing variables. These phenomena warrant significant concern due to their potential for a magnified impact on both ecosystems and human societies, an impact which typically surpasses that of isolated events. The progression of global warming suggests that extreme weather conditions, such as droughts and heatwaves—once considered historical anomalies—could become a recurrent reality (Leng et al., 2016; Morrison et al., 2019; Gudmundsson et al., 2021). Anticipated to be frequent in the decades ahead for many regions, this new normal raises the probability of more frequent compound events, possibly inducing unprecedented and catastrophic effects on society and the environment. Hence, precise evaluations of the fluctuating nature of compound drought and hot incidents are imperative. Such analyses are crucial for deepening our comprehension of these events and for the development of strategies aimed at mitigating their adverse effects.

In recent times, numerous studies have delved into the characteristics of compound drought-hot (CDH) events across diverse temporal and spatial scales. Their findings indicate a discernible uptick in the frequency of CDH events during the observed period, and projections suggest a further escalation under high future emission scenarios in most global regions (Mukherjee et al., 2019; Mukherjee and Mishra, 2021; Wu et al., 2021a, 2021b; Yuan et al., 2019). Various methodologies (Leonard et al., 2014; Mazdiyasni and AghaKouchak, 2015; Zscheischler and Seneviratne, 2017; Wu et al., 2019; Bevacqua et al., 2021) have been proposed to quantify and elucidate the characteristics and associated risks of CDH events. Some research endeavors have not only clarified but also extended the conceptual understanding of compound events. They have established a comprehensive framework for studying compound events, aiming to quantify their impacts and risks. Furthermore, to capture the essence of drought-hot climate conditions, certain studies have adopted the percentile of monthly precipitation and temperature (Wu et al., 2020; Zhou and Liu, 2018; Zscheischler and Seneviratne, 2017; Ballarin et al., 2021; Ghanbari et al., 2023), specifically focusing on low precipitation percentile and high temperature percentile. In recent years, an increasing body of literature has delved into the variation of CDH characteristics, defining CDH events as heatwave episodes occurring under drought conditions (Feng et al., 2020; Mukherjee et al., 2020; Mukherjee and Mishra, 2021). In these investigations, the Standardized Precipitation Index (SPI) or Palmer Drought Severity Index (PDSI) has been instrumental in identifying drought events. Simultaneously, a heatwave is typically delineated as a span of consecutive extremely hot days, with the daily maximum temperature (T_{max}) surpassing a predetermined percentile threshold.

Temperature and precipitation, as two fundamental components, serve as crucial indicators of the potential evolution of Earth's climate systems. A consensus has emerged, highlighting the inverse correlation between temperature and precipitation during the summer months. The mechanism underpinning land surface feedbacks, particularly influenced by soil moisture deficiency on surface temperature, stands as the primary driver behind this negative correlation (Trenberth and Shea, 2005; Seneviratne et al., 2010a, 2010b; Ribeiro et al., 2020). These feedbacks, intricately intertwined with boundary layer processes, play a pivotal role in the climate regimes that lead to the conversion between drought and wet conditions. On the land surface, the negative relationship between precipitation and temperature during the summertime emerges as a key driving force behind concurrent drought-hot events, surpassing the impact when both elements are considered independently. Consequently, this study focuses exclusively on the land surface, conducting a systematic analysis of its influence. Given the widespread ramifications of compound drought-hot events, there is a growing emphasis on quantifying and detecting dynamic variations in concurrent precipitation and temperature extremes under a warming climate. Therefore, a combined indicator encompassing multiple extremes or events assumes a pivotal role in this context. Over recent years, various joint indicators of climate extremes have emerged, designed to evaluate diverse properties, including severity and spatial extent. These indicators account for multivariate factors linked to extremes, offering a comprehensive assessment of their characteristics (Estrella and Menzel, 2012; Hao et al., 2013; Mazdiyasni and AghaKouchak, 2015; Miao et al., 2016). As an illustration, the Climate Extremes Index (CEI) has integrated multiple extremes by computing the linear average of areas covered by various extreme indicators (Gallant et al., 2014). It has been widely utilized to evaluate changes in spatial extent. The assessment of extreme event severity has also seen the application of the joint probability of multivariate random variables. For example, Hao et al. (2019) proposed the Standardized Compound Event Indicator (SCEI) to gauge the severity of compound drought and hot events by standardizing the joint probability of droughts and hot events. These joint indices serve as valuable tools, enhancing our comprehension of the frequency, spatial extent, and severity of different extremes. Although studies have been carried out employing joint indicators to evaluate the evolving trends of compound drought-hot (CDH) events, a deeper comprehension is essential regarding the ways in which climatic determinants influence the alterations in the attributes of these CDH occurrences.

In this study, we undertake a detailed analysis of the spatio-temporal variations in compound drought-hot (CDH) events across China. To encapsulate the complexity of these CDH events, we have formulated an empirical Copula-driven multivariate index which integrates the monthly Standardized Precipitation Evapotranspiration Index (SPEI) and the Standardized Temperature Index based on grid-derived observations recorded during 1901–2022. Additionally, our methodology employs a path analysis framework to scrutinize the reaction of CDH events to prominent climatic impactors, including the summer mean temperature (SuT) and the summer climatic water deficit (SuWD: the discrepancy between actual precipitation and potential evapotranspiration (PET)). This approach is

engineered to deepen our grasp of how these influential factors steer CDH events in the context of escalating global temperatures. The aims of this study are manifold: (a) to establish the multivariate index that will facilitate a historical examination of fluctuations of CDH severity in China, and (b) to appraise the influence of temperature and water scarcity on CDH events with precision.

2. Data and methods

2.1. Datasets and study area

Due to the large size of China, precipitation, potential evapotranspiration and temperature could be dramatically different in different regions of China (Fig. 1). Therefore, 9 sub-regions were selected in this study, including the Songhua and Liaohe River Basin (SLRB), Haihe River Basin (HaRB), Huaihe River Basin (HuRB), Yellow River Basin (YB), Yangtze River Basin (YRB), Pearl River Basin (PRB), Southeast Basin (SEB), Southwest Basin (SWB) and Continental Basin (CB).

In our study, we leveraged high-resolution meteorological data sourced from the Climate Research Unit (CRU), specifically focusing on monthly precipitation, potential evapotranspiration, and temperature data at a 0.5° spatial granularity. This data, accessible at CRU Data Portal, covers an extensive period from 1901–2022, as detailed in Harris et al. (2020). Utilizing this detailed grid-based meteorological dataset, we successfully developed an empirical Copula-based index, designed to accurately represent the changes of compound drought-hot events.

2.2. Methods

2.2.1. Construction of Compound drought-hot index (CDHI)

In contrast to the other frequently employed drought metrics, specifically the self-calibrated Palmer Drought Severity Index (sc-PDSI) as outlined by Wells et al. (2004), and the Standardized Precipitation Index (SPI) introduced by McKee et al. (1995), the SPEI (Standardized Precipitation Evapotranspiration Index) is deemed more adept for the identification, surveillance, and examination of drought phenomena within the context of global warming. This is attributed to SPEI's comprehensive assessment of the impact of potential evapotranspiration (PET) (which encompasses factors such as solar radiation, temperature, wind speed, air pressure, and relative humidity) on drought scenarios (Vicente-Serrano et al., 2010).

Inspired by the study of Hao et al. (2019), we employed the Standardized Precipitation Evapotranspiration Index (SPEI) (McKee et al., 1993) alongside the Standardized Temperature Index (STI) to evaluate the respective drought and hot conditions. Our attention

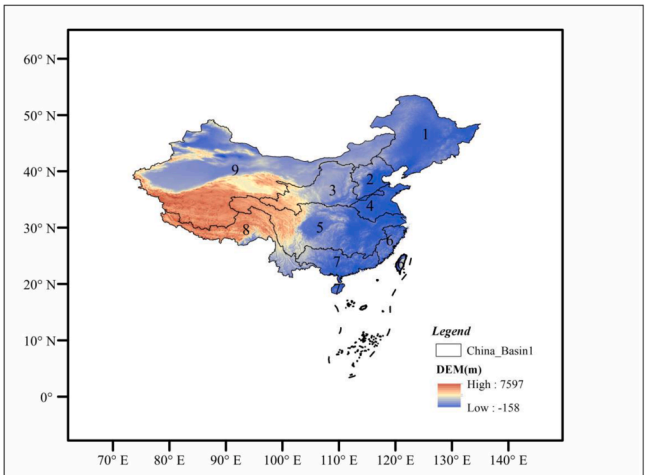

Detailed information of the classified basins in this study

No.	Name	Abbreviation
1	Songhua and Liaohe River Basin	**SLRB**
2	Haihe River Basin	**HaRB**
3	Yellow River Basin	**YB**
4	Huaihe River Basin	**HuRB**
5	Yangtze River Basin	**YRB**
6	Southeast Basin	**SEB**
7	Pearl River Basin	**PRB**
8	Southwest Basin	**SWB**
9	Continental Basin	**CB**

Fig. 1. Study area and the list of sub-regions used in this study.

centered on the summer months (June, July, and August - JJA). Therefore, we calculated the SPEI and STI using the summer mean water deficit (SuWD) and temperature (SuT) data specifically from the JJA period. To estimate the marginal distributions, we utilized the empirical Gringorten plotting position formula (Gringorten, 1963). These distributions were then converted into the SPEI and STI, aligning them with the standard normal distribution framework.

In the context of this study, we engage two stochastic variables: X, indicative of drought conditions via the Standardized Precipitation Evapotranspiration Index (SPEI), and Y, which signifies episodes of elevated temperatures, as measured by the negative Standardized Temperature Index (-STI). A compound drought-hot phenomenon is thus delineated by the concurrent manifestation of X not surpassing a specified lower boundary x, and Y concurrently not surpassing a lower limit y. To additionally account for scenarios where STI readings remain below a distinct cap, we strategized a novel method that inversely couples the variable (-STI) with the SPEI. By implementing this innovative pairing, we are equipped to calculate the joint probability (p_{CDH}) of concurrent drought-hot events:

$$p_{CDH} = P\left(X_{SPEI} < x_{SPEI}, Y_{(-STI)} < y_{(-STI)}\right) = C_n(u, v) \tag{1}$$

where u and v are marginal distributions of random variables X and Y, respectively. $C_n(u, v)$ is just the empirical copula function fitting for the dependence structure of SPEI and (-STI). Copulas stand as an indispensable tool in hydrological studies (Kao and Govindaraju, 2010; Hao and AghaKouchak, 2013), heralding a new era in the construction of joint distributions for multivariate random variables. Their utility branches out across a plethora of applications within the field, most notably in the derivation of joint extreme indicators. The employment of copulas thus provides a sophisticated lens through which the complexities of multivariate water-related events can be analyzed and understood with greater depth and clarity.

To gauge the severity of simultaneous drought and heat phenomena, we consider the joint probability, denoted as p_{CDH}, to be a significant metric. This joint probability p_{CDH} undergoes a transformation akin to the procedures utilized for generating the Standardized Precipitation Evapotranspiration Index (SPEI) and the Standardized Temperature Index (STI). Specifically, we fit joint probability p_{CDH} to a suitable distribution F, which is then adjusted to a uniform scale. This standardization enables us to employ it as a calibrated indicator that quantifies the severity of such compound drought and hot events with greater precision. The methodology we adopt effectively harmonizes the varying scales of SPEI and STI, providing a unified index that captures the essence of these concurrent climatic elements (precipitation, temperature and potential evapotranspiration). The compound drought-hot event index (CDHI) can be calculated as:

$$CDHI = \phi^{-1}[F(p_{CDH})] \tag{2}$$

We can adeptly sidestep the presumptions inherent in parametric distribution forms by fitting the marginal distribution functions, denoted as F, using the empirically-driven Gringorten plotting position formula. This nonparametric approach enables a more adaptive and potentially accurate modeling of the data, embracing its natural variability without the constraints of predetermined parametric assumptions. Similar to this idea, the empirical copula was adopted in this study to derive the joint probability of -STI and the SPEI to enhance the robustness and reliability of our distributional analysis.

Lower values of these indices are indicative of intensified severity in concurrent drought and heat events. In a manner analogous to Svoboda et al. (2002) who established threshold values for the SPI to delineate various drought intensities, we have developed a categorical system to classify the range of compound drought and hot conditions: three distinct categories: CDH1 marking an abnormal state; CDH2 indicating moderate severity; CDH2, corresponding to a severe level. The specifics of these categories are systematically articulated in Table 1, offering clear demarcation and facilitating nuanced understanding of these complex climatic phenomena.

2.2.2. Path analysis

In our exploration of compound drought-hot (CDH) events, we've adopted path analysis to understand how variations in these events might relate to changes in key influencing factors. Specifically, we focus on summer mean temperature (SuT) and summer mean water deficit (SuWD: the difference between precipitation and potential evapotranspiration (PET)). These factors are widely recognized as critical drivers of CDH events, as highlighted in previous research (Tomas-Burguera et al., 2020; Timilsina et al., 2014; Zhang et al., 2022). Path analysis, a refined version of multiple regression, is particularly adept at handling the interplay between variables. Its application is prevalent in studies seeking to quantify and understand the nature and strength of potential causal relationships, especially when the influences of different variables are intertwined (Saito et al., 2009; Smith et al., 1997; Tomas-Burguera et al., 2020; Yan et al., 2022). A notable strength of path analysis lies in its ability to break down the correlation coefficient into specific components: the direct and indirect interaction coefficients. This breakdown is invaluable, as it provides a more granular view of how direct and indirect effects contribute to the overall relationship, which is a nuance often overlooked in standard regression methods. This approach is well-documented and has been effectively utilized in recent studies (Li et al., 2019; Cheng et al., 2021; Gorai et al., 2020), underscoring its value in understanding the complex dynamics of CDH events.

Table 1
The classification system outlined in this study through Compound Dry and Hot Index (CDHI).

Category	Compound dry-hot status	Percentile	CDHI
CDH1	Abnormal	20–30	$[-0.7, -0.5]$
CDH2	Moderate	10–20	$[-1.2, -0.8]$
CDH3	Severe	< 10	-1.3 or less

Path analysis stands out in statistical methodology due to its allowance for the interdependence among variables, negating the need for strict independence that often constrains other analytical approaches. This method evaluates the path coefficients as measures of relative sensitivity, quantifying the extent to which the dependent variable, y, responds to changes in each independent variable $x_i (i = 1, 2, \ldots, n)$. By deconstructing a complex network of correlations involving a single dependent variable and multiple independents, path analysis affords us the capacity to untangle the nuanced influences within the system. These path coefficients, therefore, become definitive indicators, revealing the strength and direction of each relationship in our model. The process for isolating these influences within a correlative system is mathematically articulated by the following formula:

$$R_{yi} = P_i + r_{i1}P_1 + r_{i2}P_2 + \ldots + r_{ij}P_j \quad j = 1, 2, \ldots, n; j \neq i \tag{3}$$

where n is the number of independent variables and is equal to two in this study (i.e., SuT and SuWD). R_{yi} symbolizes the Pearson correlation coefficient between each independent variable x_i and the dependent variable y. It encompasses the full extent of influence that x_i exhibits on y. P_i refers to the direct path coefficient for x_i impacting y. It systematically encapsulates the direct effect along the trajectory from x_i to y. r_{ij} denotes the Pearson correlation coefficient relaying the relationship between two independent variables, x_i and x_j. $r_{ij}P_j$, articulated as the indirect path coefficient, captures the nuanced effect that x_i has on y, mediated through its interaction with another independent variable x_j. It quantifies the subtle and cascading impact of x_i on y, negotiating through the intermediary variable x_j. Through the application of this formula, we are afforded a comprehensive lens through which the direct and mediated impacts of the selected variables on the dependent measure can be discerned and evaluated with precision.

The determination coefficient, commonly abbreviated as *DC*, serves as a vital metric for assessing the impact exerted by related factors on a given dependent variable. This coefficient takes into account both single-factor effects and interactions between pairs of

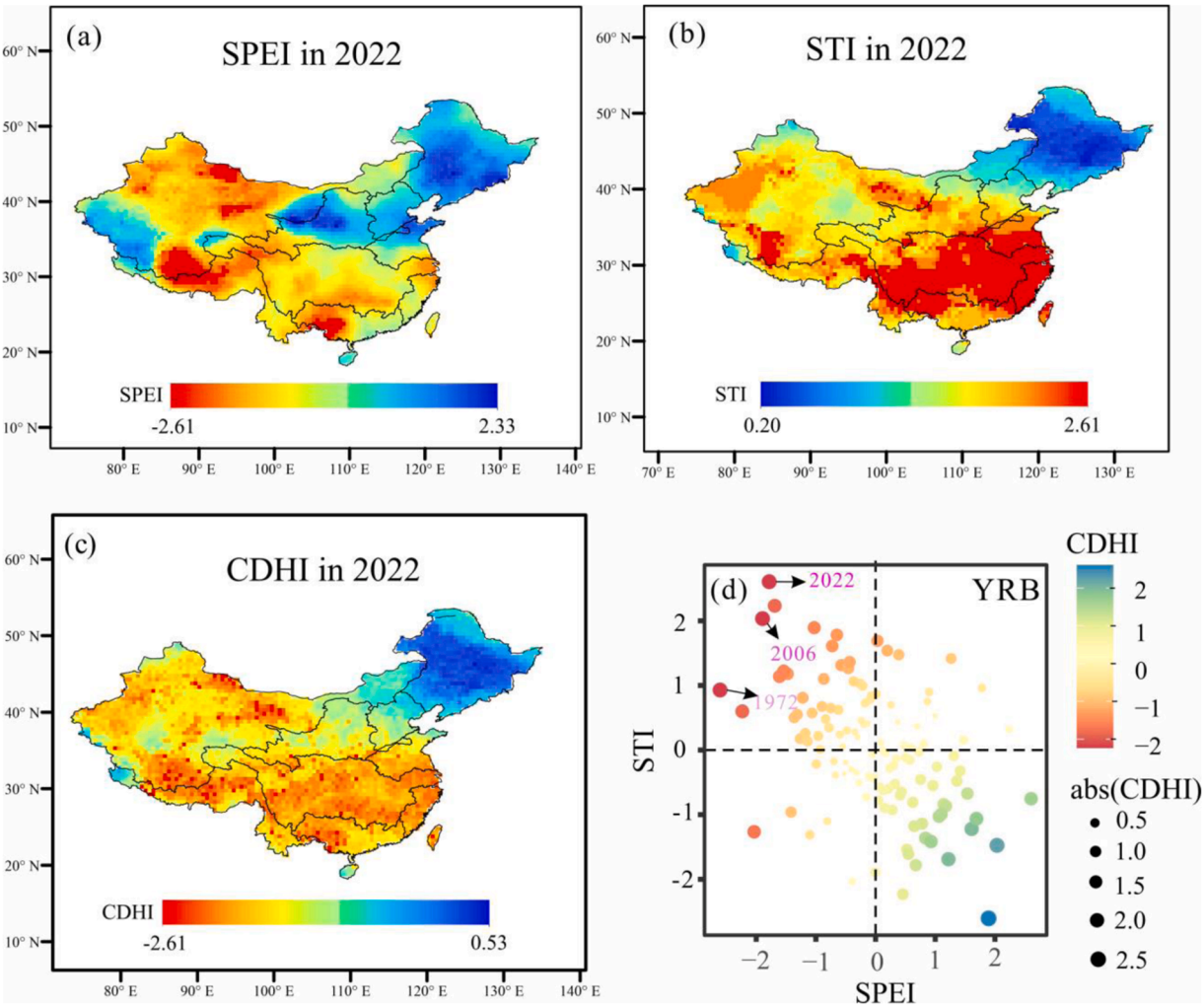

Fig. 2. The spatial distribution of the SPEI (panel a), the STI (panel b), and the CDHI (panel c) are presented across China for the summer months (June, July, August: JJA) of 2022. Additionally, panel d features a scatterplot illustrating the interrelationship between SPEI and STI as determinants of CDHI within the Yangtze River Basin (YRB).

factors. Its definition is as follows:

$$DC_i = P_i^2 \tag{4}$$

$$DC_{ij} = 2P_i r_{ij} P_j \tag{5}$$

where DC_i quantifies the extent to which the independent variable x_i directly dictates the value of the dependent variable y. Similarly, DC_{ij} represents what is known as the co-determination coefficient, indicating the collective influence of the combined independent variables x_i and x_j on the dependent variable y. DC_{tot} sums up these individual and combined contributions: the direct determination coefficients and the co-determination coefficients. To capture the unaccounted variance, we calculate the residual determination coefficient DC_{Res}, which is computed by subtracting DC_{tot} from 1. To derive a metric for the magnitude of this unexplained variance, the residual path coefficient, denoted as P_{Res}, can be found by taking the square root of DC_{Res}.

$$DC_{tot} = \sum_{i=1}^{n} DC_i + \sum_{i=1}^{n} \sum_{j>i}^{n} DC_{ij} \tag{6}$$

$$P_{Res} = \sqrt{1 - DC_{tot}} \tag{7}$$

Building upon this, our study quantifies the influence of chosen factors (i.e., SuT and SuWD) on the variability of compound drought-hot (CDH) events by deploying path coefficients. The strategy for defining the relative contribution rate is delineated below (Tomas-Burguera et al., 2020):

$$CR_i = \frac{|P_i|}{\sum_{i=1}^{n} |P_i|} \tag{8}$$

where CR_i symbolizes the relative contribution rate attributable to the influencing factor x_i. For this research, the compound drought-hot index (CDHI) is posited as the dependent variable, with SuT and SuWD serving as the independent variables. The path coefficients for SuT and SuWD are denoted as P_{SuT} and P_{SuWD}, respectively. Furthermore, the direct determination coefficients are represented as DC_{SuT} and DC_{SuWD}, encapsulating the individual impacts of SuT and SuWD on CDHI. The joint influence of these independent variables is quantified by the co-determination coefficient DC_{CO}, which measures the collective interaction between SuT and SuWD in affecting the CDHI. To substantiate the empirical significance of the path analysis outcomes, an F-test is employed (Aguilar et al., 2009; Wasserstein and Lazar, 2016). The results derived from the path analysis are deemed statistically significant if the p-value falls below the threshold of 0.05. The CR_{SuT} and CR_{SuWD} refer to the contribution rate of SuT and SuWD, respectively.

3. Results

3.1. Assessment of CDHI to monitor the historical compound drought-hot events

Considering that the majority of regions of Northern Hemisphere (NH) have experienced concurrent or consecutive occurrences of drought and hot events in 2022 (Hao et al., 2023; Tripathy and Mishra, 2023; Meng et al., 2023; Faranda et al., 2023; Tang et al., 2023), we present spatial distribution of the compound high-temperature and drought severity across China for the year 2022 based on the CDHI indicator proposed in this paper (Fig. 2). Fig. 2**(a), (b)** and **(c)** reveals that in 2022, six out of nine major river basins in China, including the Yangtze River Basin (YRB), Southeast Basin (SEB), Southwest Basin (SWB), Pearl River Basin (PRB), Huaihe River Basin (HaRB), and Continental Basin (CB), experienced compound drought and hot conditions. This was particularly acute in most areas of the YRB, where the SPEI dipped below −1, and the STI exceeded 1.8. The Compound Drought-Hot Index (CDHI) values were predominantly lower than −1.5, categorizing these conditions as more severe than the CDH3 level of compound drought and hot events. Notably, the CDHI values were lower than those of the SPEI, suggesting that high temperatures exacerbated the drought conditions, culminating in the occurrence of compound drought and hot events during the summer of 2022. This observation aligns with the findings of Tang et al. (2023), who noted that the compound drought-hot events in the Yangtze River basin led to rolling blackouts following record-high electricity demands.

Fig. 2**(d)** and Figure S2 are used to illustrate the effectiveness of the compound drought-hot index (CDHI) in evaluating the intensity of combined drought and hot conditions. These figures depict CDHI, along with the Standardized Precipitation Evapotranspiration Index (SPEI) and Standardized Temperature Index (STI), specifically during the summer months (JJA), covering a wide time span from 1901 to 2022. The analysis is focused on the Yangtze River Basin (YRB) using a river basin-centric approach. These climate indices were calculated based on the JJA mean precipitation and temperature for each year, derived from spatially averaged precipitation and temperature data collected from all grid points within the region. Fig. 2**(d)** highlights that the YRB was hit by particularly intense compound drought-hot events in the years 1972, 2006, and 2022, with the CDHI reaching a minimum of −2.33 in these three years, denoted by a stark red hue, indicating extreme severity. The grey area of Figure S2 also demonstrated this phenomenon that the increasing of STI has deduced the exacerbation of compound drought-hot events with decreasing of CDHI.

When examining the observed three most severe events at year 1972, 2006, and 2022, there appears to be a pattern where drought conditions have slightly improved, moving from −2.61 in 1972, to −1.89 in 2006, and further to −1.78 in 2022. Contrarily, the

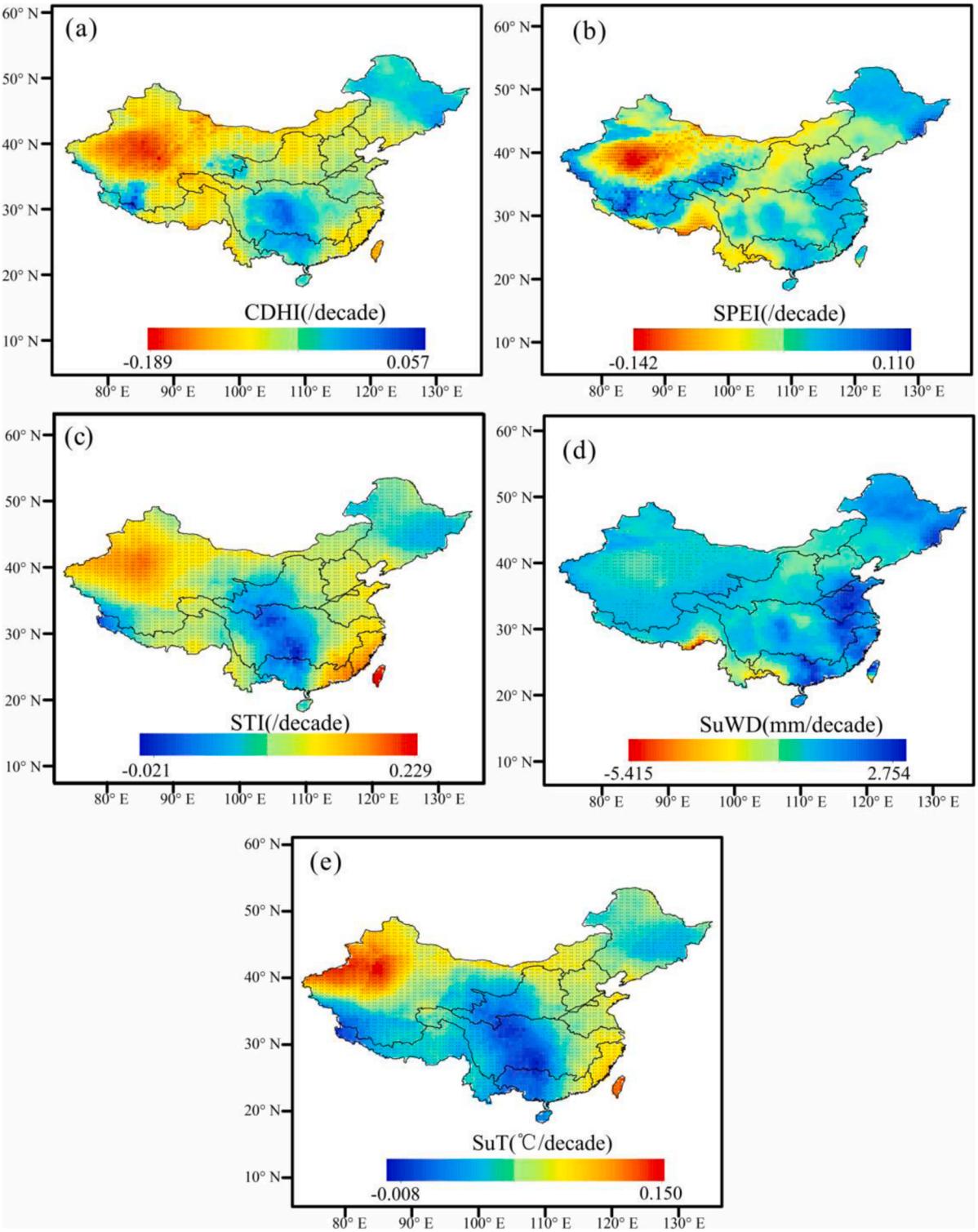

Fig. 3. The results of trend analysis for (a)CDHI, (b)SPEI, (c)STI, (d)SuWD and (e) SuT during the summer (JJA) period from 1901 to 2022 across China. To estimate these trends, we employed the nonparametric Mann-Kendall (MK) test. Trends marked with a "+" symbol represent statistical significance, satisfying the 0.05 threshold for the significance level.

intensity of heat conditions has escalated from 0.92 in 1972–2.03 in 2006, and then to 2.60 in 2022. This trend suggests that, under the influence of global warming, extreme compound drought-hot (CDH) events are increasingly likely to be driven by rising temperatures. Within the context of all nine analyzed river basins (as depicted in Fig. 2**(d)** and Figure S1), it has been observed that the most severe CDH events, as indicated by the lowest CDHI values, have become noticeably more frequent in the most recent six decades (1962–2022), in contrast to the earlier period spanning from 1901 to 1962.

While the SPEI and STI may indicate either a drought or a hot condition independently, the CDHI can provide a more comprehensive perspective by potentially revealing a compound drought-hot condition. This nuanced interpretation is crucial, as it underscores the multifaceted nature of these environmental events. For instance, the summer of 1946 of YRB presented a stark example (as shown in Figure S2): the STI was at a high of 1.96, signaling severe heat, whereas the SPEI registered at 0.48, suggesting the absence of drought conditions. Despite these individual values of SPEI and STI, the CDHI indicated a compound drought and hot condition with a value of −1.27 for that year. This scenario highlights the distinctive capability of the CDHI as a multivariate indicator in identifying compound events that might have significant impacts, even when the contributing variables are not at their extreme levels. Such insights align with the assertions of Seneviratne et al. (2010), who emphasized the importance of considering the combined effects of multiple environmental factors when assessing the severity and potential impacts of such events.

3.2. *Trend analysis of severity changes and affected areas of compound drought-hot events*

In this section, we explore the temporal changes of compound drought and hot events across China, leveraging the Compound

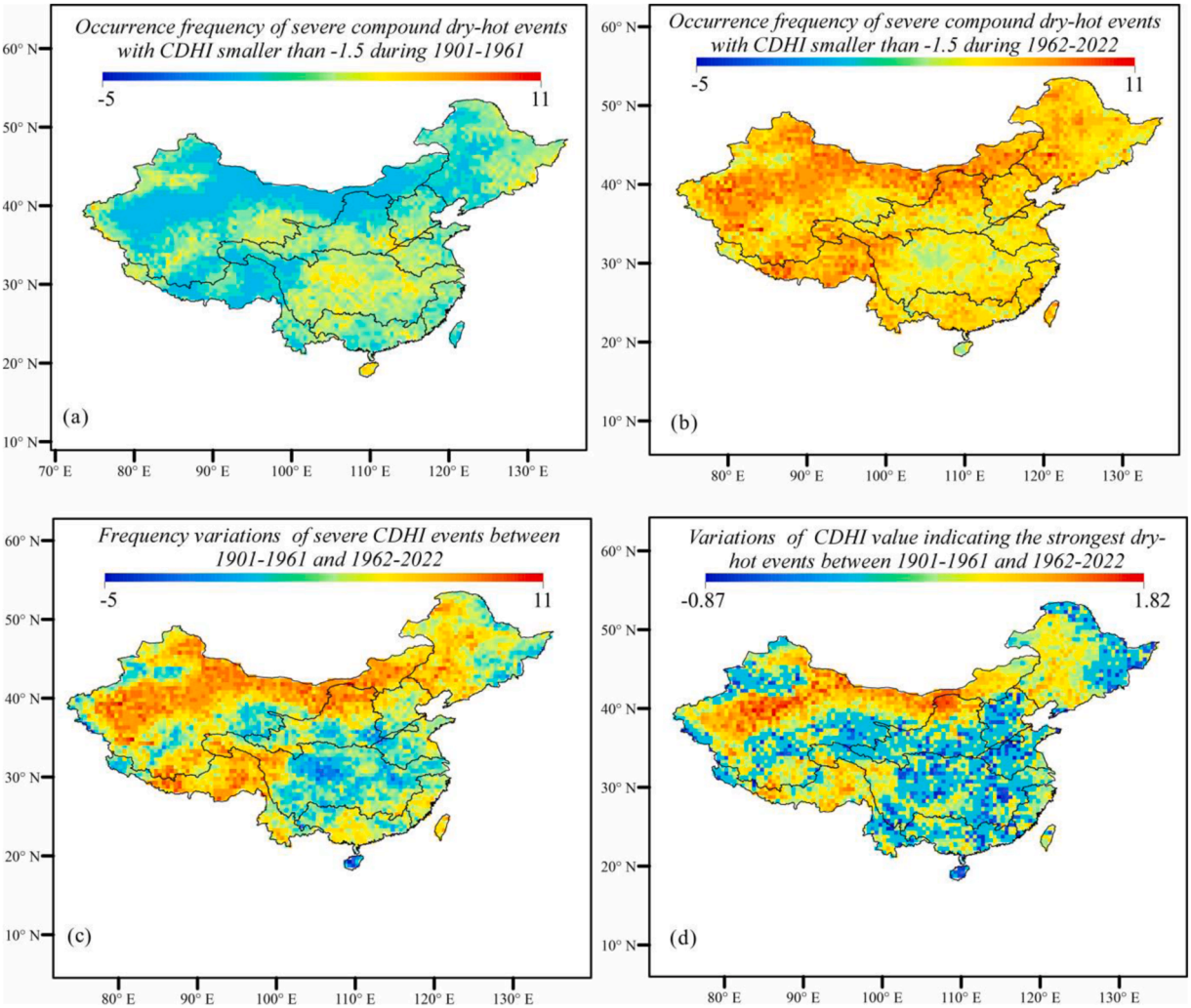

Fig. 4. Variations of occurrence frequency of the relatively severe compound dry-hot events between 1901 and 1961 and 1962–2022. (a)-(b) showed the occurrence frequency of severe compound dry-hot events with $CDHI < -1.3$ during 1901–1961 and 1962–2022, respectively. (c) indicated the frequency variations between the above two periods. (d) represented the CDHI changes denoting the strongest dry-hot events for these two periods.

Drought-Hot Index (CDHI) and applying the nonparametric Mann-Kendall (MK) trend test for an in-depth analysis. Fig. 3 offers a visual representation of these trends, showcasing the slope values from the MK test for CDHI, as well as SPEI, STI, SuWD and SuT during JJA for the period 1901–2022. Our findings reveal a nuanced geographical variance in the severity of these compound events. Notably, there's a discernible decrease in the severity (reflected as an increase in CDHI values) in central regions and some parts of northwestern China. This trend could be attributed to a combination of increased water deficit and a decrease in temperature, as delineated in Fig. 3 **(d)** and **(e)**. However, the broader picture across most parts of China paints a different scenario, where there's a marked increase in the severity of compound drought and hot events, as indicated by the CDHI. Furthermore, the trend towards increasing severity (decreasing trend of CDHI value) of compound drought and hot events is more pronounced in western China compared to eastern China. This distinction underscores a notable geographical disparity in the impact of these climatic phenomena. This observation aligns closely with existing research (Wang et al., 2016; Shi et al., 2018), which report an increased frequency of droughts and hot days in China over recent decades.

The escalating severity of compound drought and hot events can potentially be attributed to either the individual effects or the synergistic interactions of fluctuations in precipitation and temperature. For instance, should the temperature rise while the water deficit remains constant, we can anticipate an intensification of compound events. In a more localized context, decreases in water deficit have been observed in many parts of northeastern and southwestern China, which occurs concurrently with a notable uptick in temperature (as illustrated in Fig. 3**(d)** and **(e)**). Such variations in water deficit and heat conditions seem to be in harmony with the conclusions of prior research findings (Zhai et al., 2005; Lu et al., 2014). These studies collectively reinforce our understanding and

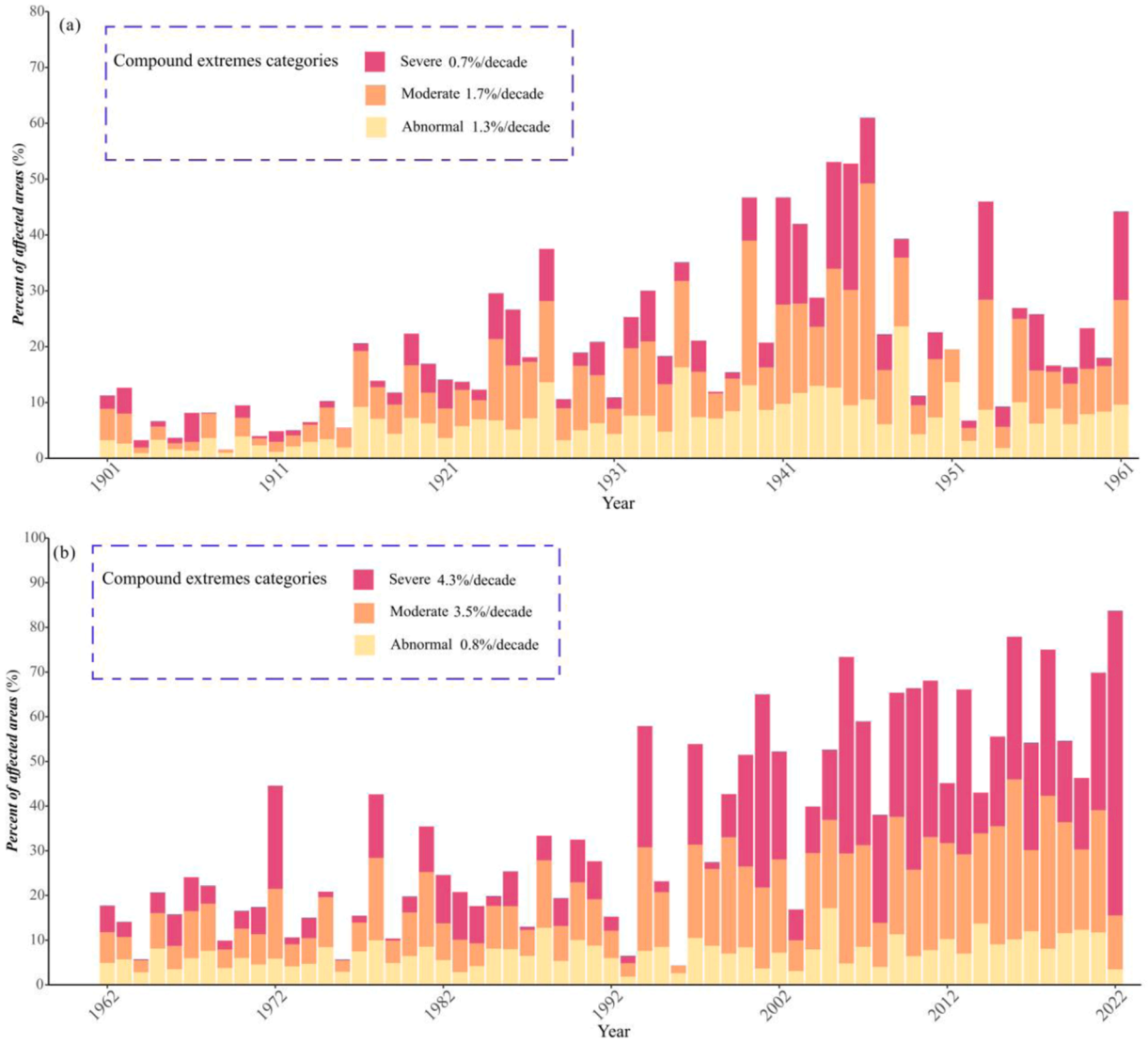

Fig. 5. Temporal trends in land area affected by varying degrees of compound dry-hot extremes during 1901–1961 and 1962–2022 at China from national scale.

provide a plausible explanation for the reported increase in the intensity and frequency of compound drought-hot events, particularly in the northeastern and southwestern regions of China. Such consistent findings highlight the necessity for comprehensive analysis to grasp the broader implications of these shifts.

The analysis of Section 3.1 has proved that more frequent compound drought-hot events had happened during the last 60 years (1962–2022) than those during 1901–1961. So, we used the gridded data to analyze the variations of occurrence frequency of the relatively severe compound drought-hot events with CDHI<-1.3 between 1901 and 1961 and 1962–2022. From Fig. 4**(a)-(c)**, it is noted that most parts of China, especially in the northeastern and southwestern areas of China, have witnessed more frequent occurrence of severe compound drought-hot events in the later 60 years (1962–2022) than former 60 years (1901–1961). Furthermore, the severity denoted by CDHI also intensified from later 60 years to former 60 years (CDHI changes denoting the strongest drought-hot events for these two periods as shown in Fig. 4**(d)**).

In this study, we define affected area as the relative coverage of areas impacted by compound drought and hot events. To categorize the severity of these events, we've selected threshold values of −0.5, −0.8, and −1.3, which represent severe, moderate, and abnormal intensity levels, respectively. We determined the spatial extent of each severity level by calculating the ratio of grid points experiencing these events to the total grid count. Our analysis is conducted at two different scales: first, we take a panoramic view at the national level, and second, we delve into the specifics at the basin level. We scrutinize the different evolving trends these compound drought-hot events across two distinct epochs—encompassing the initial 60 years from 1901 to 1961, and following up with the subsequent 60 years from 1962 to 2022. Fig. 5 illustrates the alterations in the geographical reach of compound drought and hot events across China during the summer months of June to August (JJA), segmented by the CDHI thresholds, for two key periods: 1901–1961 and 1962–2022. There's a discernible escalation in the affected areas corresponding to different severity levels, with a conspicuous intensification in the latter 60 years (1962–2022).

Delving into the finer details, the surge in both the frequency of droughts and the number of scorching days, predominantly post-1990 s, as documented by Ding et al. (2009) and Yu et al. (2014), might explain this trend. Breaking it down by category, the increments per decade in affect areas for severe, moderate, and abnormal levels during the early period (1901–1961) were 0.7%, 1.7%, and 1.3%, respectively. However, the latter period (1962–2022) witnessed a sharper climb, with the affected land area inflating by 4.3%, 3.5% corresponding to severe and moderate levels. Moreover, this pronounced trend was sharply reflected in the basin-specific analytical breakdown of the affected area displayed in the supplementary Figure S3**(a)-(b)**. These visual representations underscore the acute expansion of areas grappling with severe manifestations of compound drought-hot events over the most recent 60 years. Totally speaking, a larger part of China's land is experiencing more often and more intense compound drought-hot events because of climate warming.

3.3. Path analysis-based approach to quantify the impacts of SuT and SuWD on severity of CDH Events

Temperature and the climatic water balance play pivotal roles in the dynamics of compound drought and hot (CDH) events, due to their profound influence on heatwaves and droughts, respectively (Bevacqua et al., 2022; Zhang, Hao et al., 2022; Zscheischler and Seneviratne, 2017). Therefore, we have selected Summer Temperature (SuT) and Summer Water Deficit (SuWD) as metrics to explore how CDH severity (captured by the CDHI) responds to these climatic drivers. Recognizing the robust link between SuT and SuWD indicated in Table 2a, Table 2b, we employ path analysis to tease apart the contributions of these climate factors to the evolution of CDH events. This method allows us to disaggregate the correlation coefficients, providing nuanced insights into direct and indirect

Table 2a
Quantified effects of summer temperature (SuT) and water deficit (SuWD) on severity of CDHI events through path analysis for three periods (1901–1961, 1962–2022, 1901–2022) at SLRB, HaRB and YB River basins.

Basin	Period	Drivers	Correlation coefficient	Direct path coefficient	Indirect path coefficient	Determination coefficient	Residual path coefficient	DC_{Co}	DC_{tot}
SLRB	1901–1961	*SuT*	-0.7849	-0.5163	-0.2686	0.2666	0.2805	0.2774	0.9213*
		SuWD	0.8401	0.6143	0.2258	0.3773			
	1962–2022	*SuT*	-0.8535	-0.6506	-0.2029	0.4232	0.2993	0.2640	0.9104*
		SuWD	0.7518	0.4724	0.2794	0.2232			
	1901–2022	*SuT*	-0.8267	-0.6065	-0.2202	0.3679	0.3028	0.2671	0.9083
		SuWD	0.7782	0.5228	0.2554	0.2736			
HaRB	1901–1961	*SuT*	-0.6976	-0.5097	-0.1879	0.2598	0.2454	0.1915	0.9398*
		SuWD	0.8359	0.6989	0.1370	0.4884			
	1962–2022	*SuT*	-0.8657	-0.6828	-0.1829	0.4662	0.2152	0.2496	0.9541*
		SuWD	0.7438	0.4882	0.2556	0.2383			
	1901–2022	*SuT*	-0.7980	-0.6116	-0.1864	0.3740	0.2427	0.2280	0.9411
		SuWD	0.7781	0.5823	0.1958	0.3390			
YB	1901–1961	*SuT*	-0.8667	-0.6986	-0.1681	0.4881	0.2326	0.2349	0.9459*
		SuWD	0.7209	0.4721	0.2488	0.2229			
	1962–2022	*SuT*	-0.8195	-0.6306	-0.1889	0.3977	0.2798	0.2382	0.9217*
		SuWD	0.7574	0.5346	0.2228	0.2858			
	1901–2022	*SuT*	-0.8335	-0.6539	-0.1816	0.4276	0.2731	0.2375	0.9254*
		SuWD	0.7430	0.5103	0.2327	0.2604			

Note: the presence of the asterisk symbol "*" adjacent to the outcomes of the path analysis denotes a statistical significance level of 5%.

Table 2b
Quantified effects of summer temperature (SuT) and water deficit (SuWD) on severity of CDHI events through path analysis for three periods (1901–1961, 1962–2022, 1901–2022) at HuRB, YRB and SEB River basins.

Basin	Period	Drivers	Correlation coefficient	Direct path coefficient	Indirect path coefficient	Determination coefficient	Residual path coefficient	DC_{Co}	DC_{tot}
HuRB	1901–1961	*SuT*	-0.7892	-0.4642	-0.3250	0.2155	0.1822	0.3018	0.9668*
		SuWD	0.8954	0.6704	0.2250	0.4495			
	1962–2022	*SuT*	-0.8472	-0.7361	-0.1111	0.5418	0.2466	0.1635	0.9392
		SuWD	0.6527	0.4837	0.1690	0.2339			
	1901–2022	*SuT*	-0.8093	-0.6467	-0.1626	0.4182	0.2464	0.2104	0.9393*
		SuWD	0.7461	0.5574	0.1887	0.3107			
YRB	1901–1961	*SuT*	-0.7750	-0.5307	-0.2433	0.2816	0.3220	0.2583	0.8963*
		SuWD	0.8133	0.5970	0.2163	0.3564			
	1962–2022	*SuT*	-0.8475	-0.6078	-0.2397	0.3694	0.2805	0.2914	0.9213*
		SuWD	0.7958	0.5104	0.2854	0.2606			
	1901–2022	*SuT*	-0.8148	-0.5720	-0.2428	0.3272	0.3023	0.2778	0.9086*
		SuWD	0.8030	0.5509	0.2521	0.3035			
SEB	1901–1961	*SuT*	-0.7006	-0.3438	-0.3568	0.1181	0.2007	0.2453	0.9597*
		SuWD	0.9311	0.7722	0.1589	0.5963			
	1962–2022	*SuT*	-0.8853	-0.7076	-0.1777	0.5007	0.1913	0.2514	0.9634*
		SuWD	0.7332	0.4596	0.2736	0.2112			
	1901–2022	*SuT*	-0.8192	-0.6155	-0.2037	0.3788	0.2345	0.2508	0.9450*
		SuWD	0.7849	0.5616	0.2233	0.3154			

Note: the presence of the asterisk symbol "*" adjacent to the outcomes of the path analysis denotes a statistical significance level of 5%.

influences. In this section, our scrutiny is trained on discerning how SuT and SuWD have shaped the CDH magnitude. We are particularly attentive to the shifts in impacts from the initial 60-year span (1901–1961) to the subsequent 60 years (1962–2022). Our analysis aims to bring to light not just the present-day effects but also how the relationship between these climatic variables and CDH events has transformed over the course of a century.

Initially, our investigation focused on the influence of summer temperature (SuT) and summer water deficit (SuWD) on CDH events from an average basin angle. The results, encompassing both quantitative and graphical representations of path analysis are presented in Table 2c, Fig. 6, and the path diagram in Figure S4.

Due to the negative value of the CDHI indicator, direct path coefficient between SuT and CDHI is negative while direct path coefficient between SuWD and CDHI is positive for all nine basins analysis. Specifically, there's a negative direct path coefficient linking SuT to CDHI, implying that higher temperatures tend to exacerbate the severity of CDH events, leading to lower (more negative) CDHI values. Conversely, the positive direct path coefficient between SuWD and CDHI indicates that greater water availability serves as a mitigating factor against the severity of these events. In essence, these findings paint a clear picture: as temperatures soar, the severity of CDH events escalates, while ample water availability seems to play a crucial role in tempering this severity.

Our analysis at the national level, encapsulated in Fig. 7 through boxplots representing all land pixels across China, offers further insights. For the majority of these pixels, the path coefficient ($\boldsymbol{P_{SuT}}$) associated with SuT is negative, while $\boldsymbol{P_{SuWD}}$ for SuWD is positive.

Table 2c
Quantified effects of summer temperature (SuT) and water deficit (SuWD) on severity of CDHI events through path analysis for three periods (1901–1961, 1962–2022, 1901–2022) at PRB, SWB and CB River basins.

Basin	Period	Drivers	Correlation coefficient	Direct path coefficient	Indirect path coefficient	Determination coefficient	Residual path coefficient	DC_{Co}	DC_{tot}
PRB	1901–1961	*SuT*	-0.7369	-0.5350	-0.2019	0.2862	0.3564	0.2160	0.8730*
		SuWD	0.7863	0.6089	0.1774	0.3707			
	1962–2022	*SuT*	-0.8750	-0.6192	-0.2558	0.3834	0.2309	0.3168	0.9467
		SuWD	0.8155	0.4964	0.3191	0.2464			
	1901–2022	*SuT*	-0.8074	-0.5726	-0.2348	0.3278	0.2987	0.2689	0.9108*
		SuWD	0.8004	0.5605	0.2399	0.3142			
SWB	1901–1961	*SuT*	-0.6915	-0.5371	-0.1544	0.2885	0.3000	0.1659	0.9097*
		SuWD	0.7972	0.6748	0.1224	0.4553			
	1962–2022	*SuT*	-0.7669	-0.4909	-0.2760	0.2410	0.2835	0.2710	0.9196*
		SuWD	0.8508	0.6384	0.2122	0.4076			
	1901–2022	*SuT*	-0.7482	-0.5032	-0.2450	0.2532	0.2902	0.2467	0.9158*
		SuWD	0.8622	0.6445	0.2177	0.4158			
CB	1901–1961	*SuT*	-0.9082	-0.6255	-0.2827	0.3913	0.2218	0.3536	0.9508*
		SuWD	0.8434	0.4538	0.3896	0.2059			
	1962–2022	*SuT*	-0.9157	-0.6822	-0.2335	0.4654	0.2437	0.3186	0.9406*
		SuWD	0.7983	0.3957	0.4026	0.1565			
	1901–2022	*SuT*	-0.9104	-0.6911	-0.2193	0.4777	0.2334	0.3031	0.9455*
		SuWD	0.7793	0.4060	0.3733	0.1648			

Note: the presence of the asterisk symbol "*" adjacent to the outcomes of the path analysis denotes a statistical significance level of 5%.

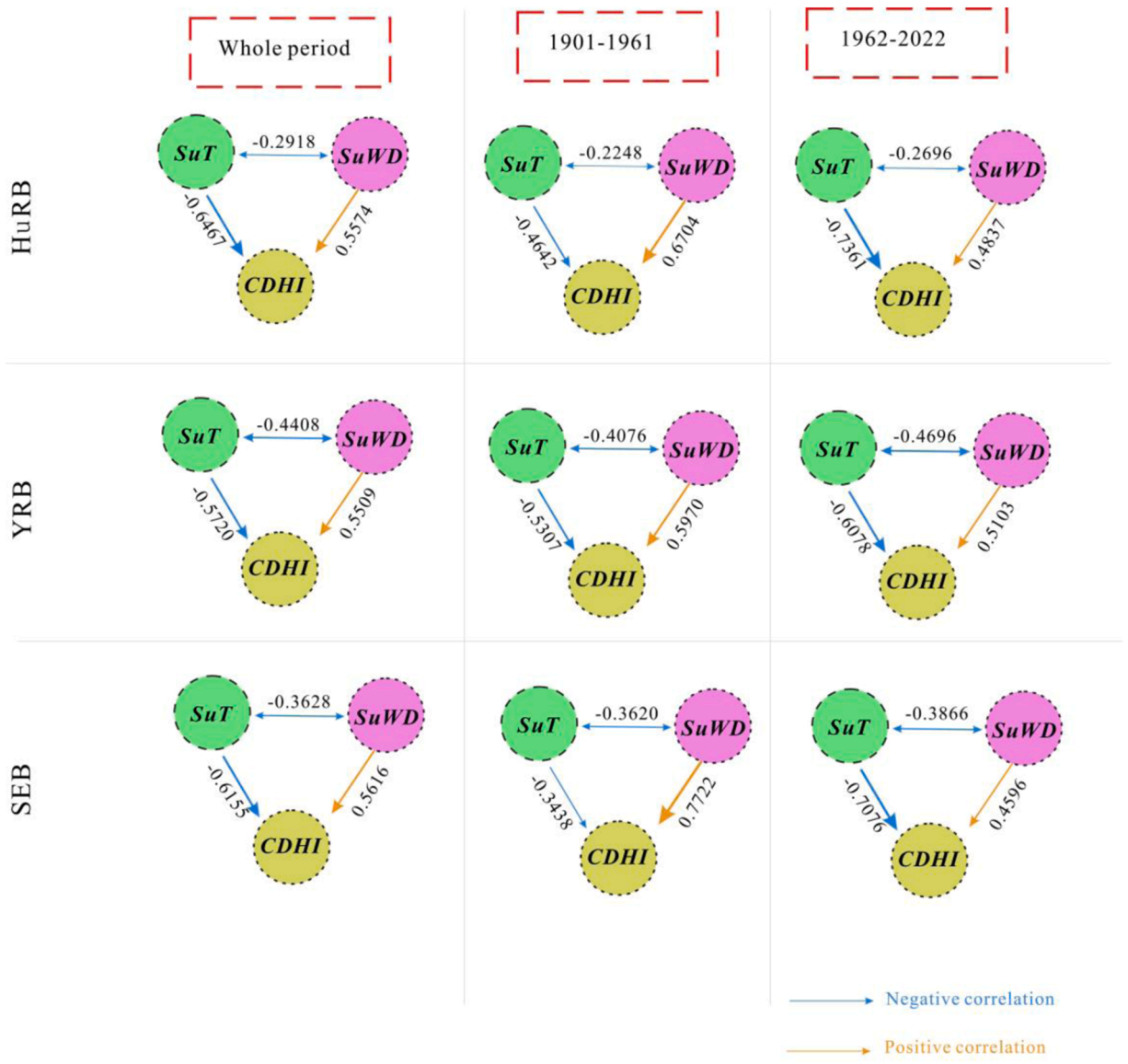

Fig. 6. Path diagrams for describing the effects of summer mean temperature (SuT) and water deficit index (Su_WD) on CDH severity under three periods (1901–1961,1962–2022, 1901–2022) for HuRB, YRB and SEB. Blue arrows represent negative effects, and earth-yellow ones are negative effect or negative correlation.

To facilitate comparison in the boxplot, we compute the absolute values of these path coefficients. A key takeaway from Fig. 7's top panel is the notable difference in the path coefficients of CDH severity relative to SuT between the two periods. It is evident that in the later timeframe of 60 years (1962–2022), the impact of SuT on the severity of compound drought-hot events is more significant in comparison to the earlier period (1901–1961). This indicates an intensifying relationship between higher temperatures and the severity of compound drought and hot events over time, underscoring the evolving nature of climatic impacts across the decades. The results of direct determination coefficient of SuT and SuWD are similar as direct path coefficients (bottom panel in Fig. 7).

Delving deeper into causes of CDH severity, we present an analysis of the contribution rate (CR) across three distinct periods: the early era from 1901 to 1961, a later phase spanning 1962–2022, as well as an overview of the entire period in question. The boxplots of the CR (Fig. 8**(d)**) correlate closely with our earlier path coefficient findings. Fig. 8 unveils a compelling trend: the impact of higher summer temperatures on CDH severity has increased in the latter 60-year period (1962–2022). This trend is quantitatively expressed through the median of contribution rates, which climbed from 0.48 in the span of 1901–1961 to a more pronounced 0.56 in the period of 1962–2022. The rise in the contribution rate of summer temperatures suggests a growing sensitivity of CDH severity to heat, a significant observation that contributes to our understanding of regional climate change trends and their environmental implications.

In line with the established definitions of $CR_{SuT}$and CR_{SuWD}, the sum of these coefficients for a specific grid always equals one

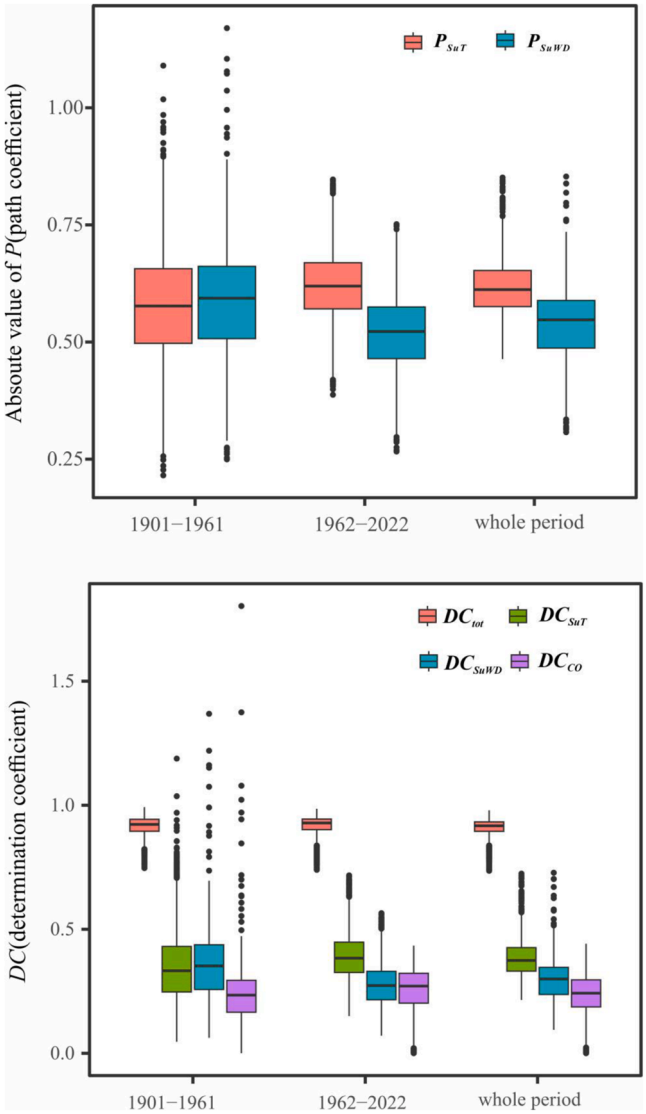

Fig. 7. Boxplot visualization of path analysis results, articulating the influence of summer temperature (SuT) and summer water deficit (SuWD) on the severity of compound dry-hot index (CDHI) across national terrestrial pixels throughout three distinct timeframes: the early century (1901–1961), the recent half-century (1962–2022), and the entire chronological span under study. Subfigure (a) delineates the path coefficients, whereas subfigure (b) details the determination coefficients. P_{SuT} and P_{SuWD} specify the direct impacts of the mean annual ***SuT*** and the annual ***SuWD*** on CDHI severity, respectively. The symbols DC_{tot}, DC_{SuT}, DC_{SuWD} and DC_{CO} quantify the total, direct, and co-determined contributions to variance explained by SuT and SuWD, respectively.

(Eq. (8)). Consequently, we have streamlined our graphical presentation to focus solely on CR_{SuT} for the illustration. For the pie chart in Fig. 8, the prominence of red signals that SuT is the prevailing factor in the evolution of CDH events when the CR_{SuT} for a given grid exceeds the 50%. Conversely, blue color in pie chart suggests that SuWD takes the lead.

From our comprehensive analysis showcased in Fig. 8**(a)-(d)**, it becomes evident that the shifts in Summer Temperature (SuT) have been the primary drivers of CDH severity changes across over 70% of China's national land during the period of 1962–2022. In contrast, the influence of Summer Water Deficit (SuWD) was more pronounced in earlier decades, dictating the CDH severity trends in 53% of the national land during 1901–1961. This shift is further emphasized in Fig. 8**(e)**, which illustrates that in eight of the nine major river basins in China, the severity of compound drought-hot events in recent years has predominantly been governed by summer temperatures.

The narrative drawn from this data is clear: the increasing temperature has been playing a more dominant role in escalating the frequency and severity of CDH events. This trend is corroborated by both the higher path coefficients of CDH characteristics to temperature and the growing contribution rate of summer temperature changes to CDH severity. This pattern, observed over the recent 60-year span, signals a marked shift in the climatic factors influencing CDH events across most regions and land pixels in China,

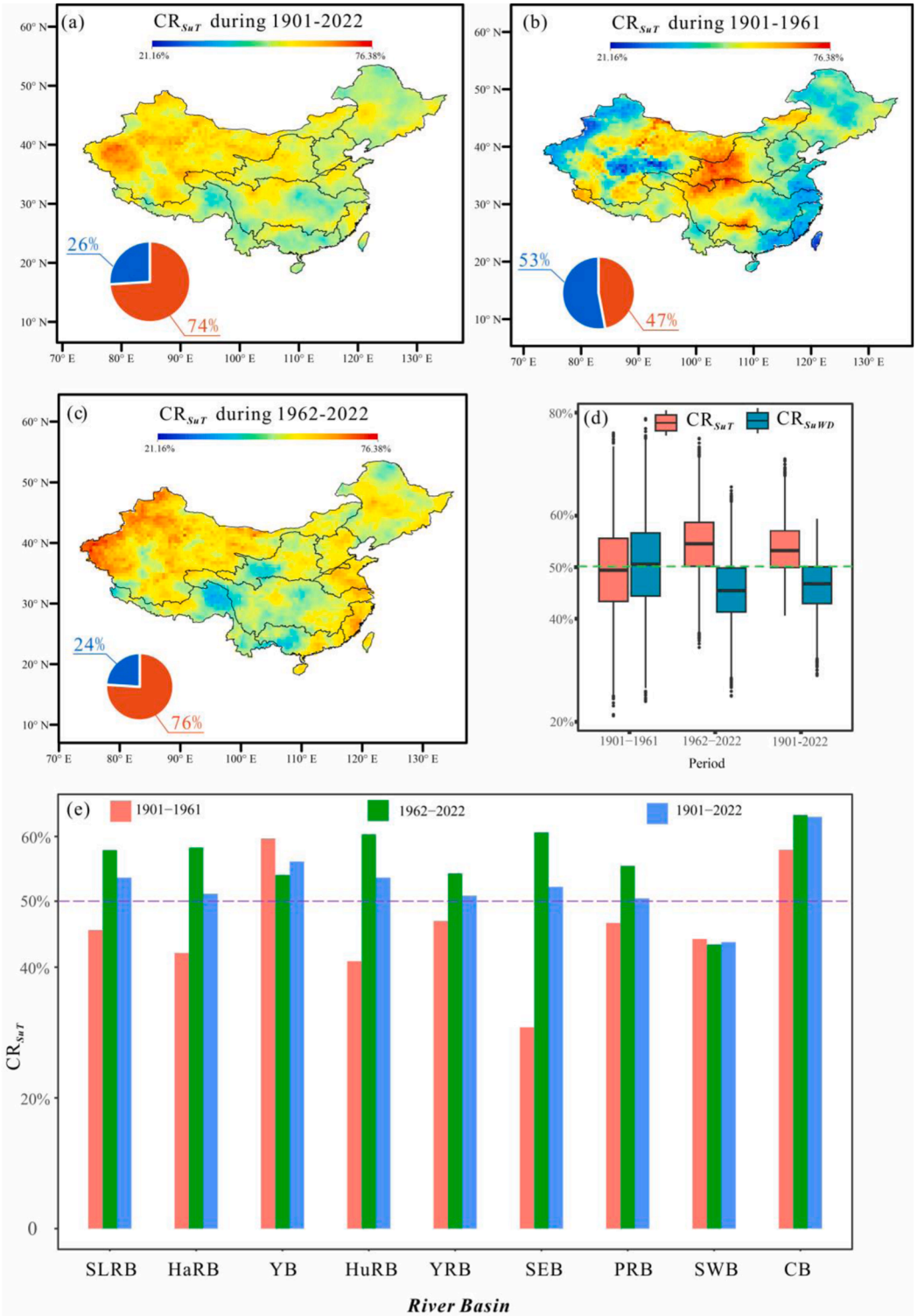

Fig. 8. Statistical features of contribution rate (CR) including **CR$_{SuT}$** and **CR$_{SuWD}$** for severity of compound dry-hot events under the whole period (1901–2022), two sub-periods (1901–1961 and 1962–2022) respectively. (a-c) spatial distributions of **CR$_{SuT}$** under three periods (whole period and two sub-periods); (d) boxplot of **CR$_{SuT}$** and **CR$_{SuWD}$** for global land areas through grid-based data; (e) The calculation of **CR$_{SuT}$** for 9 river basins in China. Pie charts depict the proportion of regions where the alteration in CDHI severity is predominantly influenced by SuT (represented in red) and SuWD (depicted in blue).

highlighting the increasing impact of temperature on the compound drought-hot events.

4. Discussion and conclusions

In this study, we have introduced an empirical-copula-based standardized compound drought-hot index (CDHI) to precisely measure and quantify the evolving intensity of compound drought-hot events (CDH) during the summertime, spanning a significant historical period from 1901 to 2022. The CDHI stands out for its ability to integrate complex climatic data, offering a clearer, more nuanced understanding of how these extreme weather events have changed over time. In our study, we delve into the intricate relationship between climate influencers, notably summer mean temperature (SuT) and summer mean water deficit (SuWD), and their impact on the changing severity of compound drought-hot (CDH) events. Our findings reveal a pronounced uptrend in the characteristics of CDH events, coupled with an increased susceptibility of these events to rising temperature across the vast expanses of China's land. However, this narrative is not without its complexities and nuances, which merit further exploration and discussion.

Leveraging the CDHI as our analytical tools, we've discerned a significant upward trend in the average traits of compound drought-hot (CDH) events, principally observable in the latter decades (as illustrated in Figs. 2–5). This trend is in consonance with prior research chronicling CDH alterations anchored in empirical observations (Hao et al., 2018; Mukherjee and Mishra, 2021). Nonetheless, we've stumbled upon certain local variations in our findings when juxtaposed with antecedent studies, discrepancies potentially attributable to variances in the data sources, the methodologies employed for identifying CDH events (Feng et al., 2020; Hao et al., 2018; Mukherjee and Mishra, 2021; Wu et al., 2019). In dissecting the 122-year timeline of our investigation into two distinct periods: the early 60 years encompassing 1901–1961, and the later 60 years extending from 1962 to 2022, we've unearthed a clear uptick in the occurrence of especially severe compound drought-hot events in the latter timeframe. This striking contrast draws attention to a mounting challenge in the recent six decades as opposed to the prior period of equal length.

Employing a path analysis framework, we've uncovered a compelling narrative: the evolution of compound drought-hot (CDH) events has been predominantly driven by escalating temperatures in the more recent six decades (1962–2022), a stark contrast to the earlier 60-year period (1901–1961). This conclusion is bolstered by two key findings: the heightened path coefficients linking CDH characteristics to temperature, and the increasingly significant role that changes in summer temperatures play in determining the severity of CDH events. In the field of climate dynamics, it's acknowledged that temperature and water deficit are interrelated phenomena (Zscheischler and Seneviratne, 2017). Generally, a rise in temperatures tends to amplify both precipitation and potential evapotranspiration (PET) (Berg et al., 2013; Kingston et al., 2009; Singleton and Toumi, 2013). Notably, in the latter 60 years of our study period (1962–2022), this interplay between summer temperature and precipitation has intensified (Table S1). This strengthening bond between temperature and water deficit is pivotal in exacerbating the frequency and intensity of compound drought-hot (CDH) events (Sarhadi et al., 2018; Zscheischler and Seneviratne, 2017). Consequently, the escalating rising temperatures emerge as a primary catalyst for the significant surge in CDH events, underscoring a crucial aspect of evolving climate narrative in China.In this study, the monthly scale-based analysis of compound dry-hot events by STI and SPEI would be too coarse to uncover the evolving regulation of short-term compound dry-hot events (Perkins and Alexander, 2013; Li et al., 2021; Hu et al., 2024). In our future study, the daily scale-based analysis of compound dry-hot events should be investigated.

The devastating effects from compound drought-hot events could induce enormous losses in ecological and social systems. Extreme high temperatures and low precipitation reduce water availability and pose a serious threat to agriculture and human health as well as an increased risk of wildfires. Considering the complexity and spatiotemporal variability of the soil moisture-temperature interactions, enhanced monitoring and model simulations are imperative to figure out their potential relationship over different climate zones in the future study.

Ethical approval

All authors kept to the ethical responsibilities of authors.

Funding

This study was supported by National Key R&D Programme of China (2023YFC3006501) and the Technical Service Project of China Yangtze Power Co. Ltd. (Z242302021).

CRediT authorship contribution statement

Xian Lin: Writing – review & editing. **Xiaoling Wu:** Writing – original draft, Formal analysis. **Hongwei Cao:** Writing – review & editing, Supervision. **Xiaohua Xiang:** Writing – review & editing, Methodology, Conceptualization. **Yongxuan Li:** Writing – review & editing, Supervision.

Declaration of Competing Interest

No conflict of interest exits in the submission of this manuscript, and manuscript is approved by all authors for publication. I would like to declare on behalf of my co-authors that the work described was original research that has not been published previously, and not under consideration for publication elsewhere, in whole or in part. All the authors listed have approved the manuscript that is

enclosed.

Data Availability

Data will be made available on request.

Acknowledgments

Gridded meteorological data used in this article are derived from the Climate Research Unit. (https://crudata.uea.ac.uk/cru/data/hrg/cru_ts_4.07/).

Appendix A. Supporting information

Supplementary data associated with this article can be found in the online version at doi:10.1016/j.ejrh.2024.101769.

References

AghaKouchak, A., Mirchi, A., Madani, K., Di Baldassarre, G., Nazemi, A., Alborzi, A., Anjileli, H., Azarderakhsh, M., Chiang, F., Hassanzadeh, E., Huning, L.S., Mallakpour, I., Martinez, A., Mazdiyasni, O., Moftakhari, H., Norouzi, H., Sadegh, M., Sadeqi, D., Van Loon, A.F., Wanders, N., 2021. Anthropogenic drought: Definition, challenges, and opportunities. Rev. Geophys. 59, e2019RG000683.

Aguilar, E., Barry, A.A., Brunet, M., Ekang, L., Fernandes, A., Massoukina, M., Mbah, J., Mhandam, A., do Nascimento, D.J., Peterson, T.C., Umba, O.T., Tomou, M., Zhang, X., 2009. Changes in temperature and precipitation extremes in Western central Africa, Guinea Conakry, and Zimbabwe, 1955-2006. J. Geophys. Res.: Atmospheres 114 (2), D02115.

Alizadeh, M.R., Adamowski, J., Nikoo, M.R., AghaKouchak, A., Dennison, P., Sadegh, M., 2020. A century of observations reveals increasing likelihood of continental-scale compound dry-hot extremes. Sci. Adv. 6, eaaz4571.

Ballarin, A.S., Barros, G.L., Cabrera, M.C.M., Wendland, E.C., 2021. A copula-based drought assessment framework considering global simulation models. J. Hydrol.: Reg. Stud. 38, 100970.

Berg, P., Moseley, C., Haerter, J.O., 2013. Strong increase in convective precipitation in response to higher temperatures. Nat. Geosci. 6 (3), 181–185.

Bevacqua, E., De Michele, C., Manning, C., Couasnon, A., Ribeiro, A.F.S., Ramos, A.M., Vignotto, E., Bastos, A., Blesić, S., Durante, F., Hiller, J., Oliveira, S.C., Pinto, J. G., Ragno, E., Rivoire, P., Saunders, K., van der Wiel, K., Wu, W., Zhang, T., Zscheischler, J., 2021. Guidelines for studying diverse types of compound weather and climate events. Earth'S. Future 9 (11), e2021EF002340.

Cheng, M., Jiao, X., Jin, X., Li, B., Liu, K., Shi, L., 2021. Satellite time series data reveal interannual and seasonal spatiotemporal evapotranspiration patterns in China in response to effect factors. Agric. Water Manag. 255, 107046.

Ding, T., Qian, W., Yan, Z., 2009. Changes in hot days and heat waves in China during 1961–2007. Int. J. Climatol. 30, 1452–1462.

Estrella, N., Menzel, A., 2012. Recent and future climate extremes arising from changes to the bivariate distribution of temperature and precipitation in Bavaria, Germany. Int. J. Climatol. 33, 1687–1695.

Faranda, D., Pascale, S., Bulut, B., 2023. Persistent anticyclonic conditions and climate change exacerbated the exceptional 2022 European-Mediterranean drought. Environ. Res. Lett. 18 (3), 034030.

Feng, S., Wu, X., Hao, Z., Hao, Y., Zhang, X., Hao, F., 2020. A database for characteristics and variations of global compound dry and hot events. Weather Clim. Extrem. 30, 100299.

Gallant, A.J.E., Karoly, D.J., Gleason, K.L., 2014. Consistent trends in a modified climate extremes index in the United States, Europe, and Australia. J. Clim. 27 (4), 1379–1394.

Ghanbari, M., Arabi, M., Georgescu, M., Broadbent, A.M., 2023. The role of climate change and urban development on compound dry-hot extremes across US cities. Nat. Commun. 14, 3509.

Gorai, A.K., Raval, S., Patra, A.K., 2020. Path analysis approach to quantify the causal factors of ground-level ozone concentration near coal-mining regions. Int. J. Environ. Sci. Technol. 17, 645–660.

Griffin, D., Anchukaitis, K.J., 2014. How unusual is the 2012–2014 California drought? Geophys. Res. Lett. 41 (24), 9017–9023.

Gringorten, I.I., 1963. A plotting rule for extreme probability paper. J. Geophys. Res. 68 (3), 813–814.

Gudmundsson, L., Boulange, J., Do, H.X., Gosling, S.N., Grillakis, M.G., Koutroulis, A.G., Leonard, M., Liu, J., Schmied, H.M., Papadimitriou, L., Pokhrel, Y., Seneviratne, S.I., Satoh, Y., Thiery, W., Wstra, S., Zhang, X., Zhao, F., 2021. Globally observed trends in mean andextreme river flow attributed to climate change. Science 371 (6534), 1159–1162.

Hao, Z., AghaKouchak, A., 2013. Multivariate Standardized Drought Index: A parametric multi-index model. Adv. Water Resour. 57, 12–18.

Hao, Z., AghaKouchak, A., Phillips, T.J., 2013. Changes in concurrent monthly precipitation and temperature extremes. Environ. Res. Lett. 8 (3), 034014.

Hao, Z., Hao, F., Singh, V.P., Zhang, X., 2018. Changes in the severity of compound drought and hot extremes over global land areas. Environ. Res. Lett. 13 (12), 124022.

Hao, Z., Hao, F., Singh, V.P., Zhang, X., 2019. Statistical prediction of the severity of compound dry-hot events based on El Niño-Southern Oscillation. J. Hydrol. 572, 243–250.

Hao, Z., Chen, Y., Feng, S., Liao, Z., An, N., Li, P., 2023. The 2022 Sichuan-Chongqing spatio-temporally compound extremes: a bitter taste of novel hazards. Sci. Bull. 68 (13), 1337–1339.

Harris, I., Osborn, T.J., Jones, P., Lister, D., 2020. Version 4 of the CRU TS monthly high-resolution gridded multivariate climate dataset. Sci. Data 7, 109.

Hu, Y., Wang, W., Wang, P., Teuling, A.J., Zhu, Y., 2024. Spatial-temporal variations and drivers of the compound dry-hot event in China. Atmospheric Research 299, 107160.

Kao, S.C., Govindaraju, R.S., 2010. A copula-based joint deficit index for droughts. J. Hydrol. 380 (1–2), 121–134.

Kingston, D.G., Todd, M.C., Taylor, R.G., Thompson, J.R., Arnell, N.W., 2009. Uncertainty in the estimation of potential evapotranspiration under climate change. Geophys. Res. Lett. 36 (20), L20403.

Kirono, D.G.C., Hennessy, K.J., Grose, M.R., 2017. Increasing risk of months with low rainfall and high temperature in southeast Australia for the past 150 years. Clim. Risk Manag. 16, 10–21.

Leng, G.Y., Tang, Q.H., Huang, S.Z., Zhang, X.J., 2016. Extreme hot summers in China in the CMIP5 climate models. Clim. Change 135 (3–4), 669–681.

Leonard, M., Westra, S., Phatak, A., Lambert, M., Van den Hurk, B., Mcinnes, K., et al., 2014. A compound event framework for understanding extreme impacts. Wiley Interdiscip. Rev.: Clim. Change 5 (1), 113–128.

Li, X., Long, D., Han, Z., Scanlon, B.R., Sun, Z., Han, P., Hou, A., 2019. Evapotranspiration estimation for Tibetan plateau headwaters using conjoint terrestrial and atmospheric water balances and multisource remote sensing. Water Resour. Res. 55, 8608–8630.
Li, J., Wang, Z., Wu, X., Zscheishler, J., Guo, S., Chen, X., 2021. A standardized index for assessing sub-monthly compound dry and hot conditions with application in China. Hydrology and earth system sciences 25, 1587–1601.
Lu, E., Zeng, Y., Luo, Y., Ding, Y., Zhao, W., Liu, S., Gong, L., Jiang, Y., Jiang, Z., Chen, H., 2014. Changes of summer precipitation in China: The dominance of frequency and intensity and linkage with changes in moisture and air temperature. J. Geophys. Res.: Atmospheres 119 (22), 12575–12587.
Mazdiyasni, O., AghaKouchak, A., 2015. Substantial increase in concurrent droughts and heatwaves in the United States. Proc. Natl. Acad. Sci. USA 112, 11484–11489.
McKee, T.B., Doesken, N.J., Doesken, J., 1995. Drought monitoring with multiple time scales. Proc. 9th Conf. Appl. Climatol. 233–236.
Meng, Y., Hao, Z., Zhang, Y., Feng, S., 2023. The 2022-like compound dry and hot extreme in the Northern Hemisphere: Extremeness, attribution, and projection. Atmos. Res. 295, 107009.
Miao, C., Sun, Q., Duan, Q., Wang, Y., 2016. Joint analysis of changes in temperature and precipitation on the loess plateau during the period 1961-2011. Clim. Dyn. 47, 3221–3234.
Morrison, A., Villarini, G., Zhang, W., Scoccimarro, E., 2019. Projected changes in extreme precipitation at sub-daily and daily time scales. Glob. Planet. Change 182, 103004.
Mukherjee, S., Mishra, A.K., 2021. Increase in compound drought and heatwaves in a warming world. Geophys. Res. Lett. 48, e2020GL09061.
Mukherjee, S., Ashfaq, M., Mishra, A.K., 2020. Compound drought and heatwaves at a global scale: The role of natural climate variability-associated synoptic patterns and land-surface energy budget anomalies. J. Geophys. Res.: Atmospheres 125 (11), e2019JD031943.
Perkins, S.E., Alexander, L.V., 2013. On the Measurement of Heat Waves. Journal of Climate 26, 4500–4517.
Ribeiro, A.F.S., Russo, A., Gouveia, C.M., Pires, C.A.L., 2020. Drought-related hot summers: A joint probability analysis in the iberian peninsula. Weather Clim. Extrem. 30, 100279.
Saito, M., Kato, T., Tang, Y., 2009. Temperature controls ecosystem CO2 exchange of an alpine meadow on the northeastern Tibetan Plateau. Glob. Change Biol. 15 (1), 221–228.
Sedlmeier, K., Feldmann, H., Schädler, G., 2017. Compound summer temperature and precipitation extremes over central Europe. Theor. Appl. Climatol. 131 (3–4), 1493–1501.
Seneviratne, S.I., Corti, T., Davin, E.L., Hirschi, M., Jaeger, E.B., Lehner, I., Orlowsky, B., Teuling, A.J., 2010b. Investigating soil moisture–climate interactions in a changing climate: a review. Earth-Sci. Rev. 99 (3–4), 125–161.
Seneviratne, S.I., Corti, T., Davin, E.L., Hirschi, M., Jaeger, E.B., Lehner, I., Orlowsky, B., Teuling, A.J., 2010a. Investigating soil moisture–climate interactions in a changing climate: A review. Earth Sci. Rev. 99, 125–161.
Shi, J., Cui, L., Ma, Y., Du, H., Wen, K., 2018. Trends in temperature extremes and their association with circulation patterns in China during 1961–2015. Atmos. Res. 212, 259–272.
Singleton, A., Toumi, R., 2013. Super-Clausius-Clapeyron scaling of rainfall in a model squall line. Q. J. R. Meteorol. Soc. 139 (671), 334–339.
Smith, F.A., Brown, J.H., Valone, T.J., 1997. Path analysis: A critical evaluation using long-term experimental data. Am. Nat. 149 (1), 29–42.
Svoboda, M., Lecomte, D., Hayes, M., Heim, R., Gleason, K., Angel, J., Rippey, B., Tinker, R., Palecki, M., Stooksbury, D., Miskus, D., Stephens, S., 2002. The drought monitor. Bull. Am. Meteorol. Soc. 83 (8), 1181–1190.
Tang, S., Qiao, S., Wang, B., Liu, F., Feng, T., Yang, J., He, M., Chen, D., Cheng, J., Feng, G., Dong, W., 2023. Linkages of unprecedented 2022 Yangtze River Valley heatwaves to Pakistan flood and triple-dip La Nina. npj Clim. Atmos. Sci. 6 (1), 67.
Timilsina, N., Escobedo, F.J., Staudhammer, C.L., Brandeis, T., 2014. Analyzing the causal factors of carbon stores in a subtropical urban forest. Ecol. Complex. 20 (20)), 23–32.
Tomas-Burguera, M., Vicente-Serrano, S.M., Pena-Angulo, D., Dominguez-Castro, F., Noguera, I., El-Kenawy, A., 2020. Global characterization of the varying responses of the standardized precipitation evapotranspiration index to atmospheric evaporative demand. J. Geophys. Res.: Atmospheres 125 (17), 1–14.
Trenberth, K.E., Shea, D.J., 2005. Relationships between precipitation and surface temperature. Geophys. Res. Lett. 32, L14703.
Tripathy, K.P., Mishra, A.K., 2023. How unusual is the 2022 European compound drought and heatwave event? Geophys. Res. Lett. 50 (15), e2023GL105453.
Vicente-Serrano, S.M., Begueria, S., Lopez-Moreno, J.I., 2010. A multiscalar drought index sensitive to global warming: The standardized precipitation evapotranspiration index. J. Clim. 23 (7), 1696–1718.
Wang, L., Yuan, X., Xie, Z., Wu, P., Li, Y., 2016. Increasing flash droughts over China during the recent global warming hiatus. Sci. Rep. 6, 30571.
Wasserstein, R.L., Lazar, N.A., 2016. The ASA's statement on p-values: Context, process, and purpose. Am. Stat. 70 (2), 129–133.
Wells, N., Goddard, S., Hayes, M.J., 2004. A self-calibrating Palmer drought severity index. J. Clim. 17 (12), 2335–2351.
Wu, H., Su, X., Singh, V.P., 2021b. Blended Dry and Hot Events Index for monitoring dry-hot events over global land areas. Geophys. Res. Lett. 48, e2021GL096181.
Wu, X., Hao, Z., Hao, F., Singh, V.P., Zhang, X., 2019. Dry-hot magnitude index: A joint indicator for compound event analysis. Environ. Res. Lett. 14 (6), 64017.
Wu, X., Hao, Z., Tang, Q., Singh, V.P., Zhang, X., Hao, F., 2020. Projected increase in compound dry and hot events over global land areas. Int. J. Climatol. 41 (1), 393–403.
Wu, X., Hao, Z., Hao, F., Zhang, X., Singh, V.P., Sun, C., 2021a. Influence of large-scale circulation patterns on compound dry and hot events in China. J. Geophys. Res.: Atmospheres 126, e2020JD033918.
Xu, P., Zhang, Z., Wang, D., Singh, V.P., Zhang, C., Fu, X., Wang, L., 2023b. A time-varying Copula-based appraoch to quantify the effects of antecedent drought on hot extremes. J. Hydrol. 627, 130418.
Xu, P., Wang, D., Wang, Y., Singh, V.P., Qiu, J., Wu, J., Zhang, A., Ju, X., 2023a. Dynamic identification and risk analysis of compound dry-hot events considering nonstationarity. J. Hydrol. 616, 128852.
Yan, R., Li, L., Gao, J., Huang, J., 2022. Exploring the influence of seasonal cropland abandonment on evapotranspiration and water resources in the humid lowland region, southern China. Water Resour. Res. 58 (4), e2021WR031888.
Yu, M., Li, Q., Hayes, M.J., Svoboda, M.D., Heim, R.R., 2014. Are droughts becoming more frequent or severe in China based on the Standardized Precipitation Evapotranspiration Index: 1951–2010? Int. J. Climatol. 34 (3), 545–558.
Yuan, X., Wang, L., Wu, P., Ji, P., Sheffield, J., Zhang, M., 2019. Anthropogenic shift towards higher risk of flash drought over China. Nat. Commun. 10, 4661.
Yuan, X., Wang, Y.M., Ji, P., Wu, P., Sheffield, J., Otkin, J.A., 2023. A global transition to flash droughts under climate change. Science 380, 187–191.
Zamora-Reyes, D., Black, B., Trouet, V., 2022. Enhanced winter, spring and summer hydroclimate variability across California from 1940 to 2019. Int. J. Climatol. 42 (9), 4940–4952.
Zhai, P.M., Zhang, X.B., Wan, H., Pan, X.H., 2005. Trends in total precipitation and frequency of daily precipitation extremes over China. J. Clim. 18 (7), 1096–1108.
Zhang, Y., Hao, Z., Feng, S., Zhang, X., Hao, F., 2022. Changes and driving factors of compound agricultural droughts and hot events in eastern China. Agric. Water Manag. 263, 107485.
Zscheischler, J., Seneviratne, S.I., 2017. Dependence of drivers affects risks associated with compound events. Sci. Adv. 3, e1700263.
Zscheischler, J., Westra, S., van den Hurk, B.J.J.M., Seneviratne, S.I., Ward, P.J., Pitman, A., AghaKouchak, A., Bresch, D.N., Leonard, M., Wahl, T., Zhang, X., 2018. Future climate risk from compound events. Nat. Clim. Change 8, 469–477.